Asymmetric Heat Transfer with Linear Conductive Metamaterials

Yishu Su,[1,†] Ying Li,[2,3,†] Minghong Qi,[2,3,†] Sebastien Guenneau,[4] Huagen Li,[5] and Jian Xiong[1,*]

[1] *Center for Composite Materials and Structures, Harbin Institute of Technology Harbin 150001, China*
[2] *Interdisciplinary Center for Quantum Information, State Key Laboratory of Extreme Photonics and Instrumentation, ZJU-Hangzhou Global Scientific and Technological Innovation Center, Zhejiang University, Hangzhou 310027, China*
[3] *International Joint Innovation Center, Key Lab. of Advanced Micro/Nano Electronic Devices & Smart Systems of Zhejiang, The Electromagnetics Academy of Zhejiang University, Zhejiang University, Haining 314400, China*
[4] *UMI 2004 Abraham de Moivre-CNRS, Imperial College London, London SW7 2AZ, United Kingdom*
[5] *Department of Electrical and Computer Engineering, National University of Singapore, Singapore 117583, Singapore*

(Received 29 March 2022; revised 1 July 2023; accepted 18 August 2023; published 7 September 2023)

Asymmetric heat-transfer systems, often referred to as thermal diodes or thermal rectifiers, have garnered increasing interest due to their wide range of application possibilities. Most of those previous macroscopic asymmetric thermal devices either resort to nonlinear thermal conductivities with strong temperature dependence that may be quite limited by or fixed in natural materials or rely on active modulation that necessitates auxiliary energy payloads. Here, we establish a straightforward strategy of passively realizing asymmetric heat transfer with linear conductive materials. The strategy also introduces an interrogative perspective into the previous design of passive asymmetric heat transfer utilizing nonlinear thermal conductivity, correcting the misconception that thermal rectification is impossible with separable nonlinear thermal conductivity. The nonlinear-perturbation mode can be versatilely engineered to produce an effective and wide-ranging perturbation in heat conduction, which imitates and bypasses intrinsic thermal nonlinearity constraints set by naturally occurring counterparts. Independent experimental characterizations of surface thermal radiation and thermal convection verify that heat exchange between a graded linear thermal metamaterial and the ambient surroundings can be tailored to achieve macroscopic asymmetric heat transfer. Our work is envisaged to inspire conceptual models for heat-transfer control, serving as a robust and convenient platform for advanced thermal management and thermal computation.

DOI: 10.1103/PhysRevApplied.20.034013

I. INTRODUCTION

The development of asymmetric heat-transfer devices, which can be treated as the counterparts of nonlinear solid-state devices regulating electrical conduction, such as diodes and transistors, has profound implications for thermal circuits and thermal management. Recently, the ability to manipulate phononic [1–6] and electronic [7–10] heat conduction has been demonstrated and offers a promising method of controlling heat flux. Thermal diodes [1,2], thermal transistors [3], thermal memory [4], and thermal circuits [11,12] at the nanoscale have been experimentally or theoretically demonstrated. At the macroscale, given the lack of conceptual underpinnings, the design of thermal-rectifier devices based on nonlinear materials is plagued by several misunderstandings, and it is also impossible to achieve asymmetric heat transfer using linear materials, and thus, passive or active asymmetric heat-transfer systems have to be achieved by employing nonlinear materials [13–16] or spatiotemporal modulations [17–19]. The thermal conductivities of natural materials often do not have strong temperature dependences, so asymmetry can only be accomplished with the aid of extra designs using shape-memory alloys [20,21] or other phase-change materials [22,23]. One of the primary reasons for this is the absence of an overarching theoretical framework for the use of alternative mechanisms.

It is now conceivable to manipulate heat flow following human desires via artificial materials and structures [24–28]. For example, one can use specialized thermal-conductivity arrangements to direct heat flow to achieve thermal cloaking [29–32], camouflaging [33–35], or transparency [36–39] in the field of heat conduction. Moreover, some studies have addressed heat convection [40–43], heat radiation [44], and the combination of these two

*jx@hit.edu.cn
†Y. Su, Y. Li, and M. Qi contributed equally to this work.

phenomena at the same time [45] related to heat conduction, which has facilitated the development of thermal metamaterials. However, their experimental implementation is still challenging, particularly the independently accurate determination of the effect of surface thermal radiation during heat conduction and the efficient characterization of out-of-plane thermal convection that eliminates the influence of thermal radiation.

Here, we establish a straightforward strategy for passively realizing asymmetric heat transfer with linear conductive materials, bypassing the limitation of nonlinear thermal conductivity. Nonlinear perturbation introduces a more general way to achieve asymmetric heat transfer without relying on nonlinear materials or active energy input. In addition to the interpretation of equivalent nonlinear parameters, it can be flexibly tailored to the conservative or nonconservative heat-transfer behavior of the system, such as in volumetric radiation or convection heat transfer or surface radiation or convection heat exchange. We experimentally verify that heat exchange caused by surface thermal radiation and thermal convection between a graded linear thermal metamaterial and the ambient surroundings can be tailored to achieve macroscopic asymmetric heat transfer.

I. NONLINEAR-PERTURBATION MODEL

In a two-terminal system, it amounts to applying a coordinate transformation, $x' = L - x$, to the heat-conduction equation, which only affects the equation along the x axis when heat flows into the system from the left and right sides. No matter how linear the thermal-conductivity distribution is, when the system is in a steady state, the temperature distribution is always symmetrical. Here, an asymmetric heat-transfer system's excogitation theory is introduced, which enables a different viewpoint and a more comprehensive understanding and scrutiny of the asymmetric heat-transport processes resulting from nonlinear materials, correcting previous misconceptions that thermal rectification is impossible with separable nonlinear thermal conductivity [15] and enabling the construction of asymmetric heat transfer by employing linear conductive metamaterials. By adding a nonlinear perturbation to the heat-conduction equation, it is possible to get asymmetric heat transfer without using a material with nonlinear thermal conductivity. The graded linear thermal metamaterials, which can induce parameter mismatches in nonlinearized equations, are used to break the fundamental symmetry. The macroscopic asymmetric heat-transfer system is experimentally demonstrated utilizing graded thermal metamaterials with an optimal gradient distribution and tailoring surface thermal radiation in the vacuum chamber and quantitatively characterized surface thermal convection.

Unlike traditional asymmetric heat-transfer systems (Fig. 1) in need of a nonlinear material, nonlinear perturbation, $\Phi(x, T, dT/dx, d^2T/dx^2, \cdots)$, containing both spatial element x and temperature T and its derivative elements, is incorporated into the heat-conduction equation to investigate the potential of breaking the symmetry in the heat-conduction process [Fig. 1(c)]:

$$\frac{d}{dx}\left(\kappa(x)\frac{dT}{dx}\right) + \Phi\left(x, T, \frac{dT}{dx}, \frac{d^2T}{dx^2}, \cdots\right) = 0. \quad (1)$$

The boundary conditions remain $T_{\text{left}} = T_H$ and $T_{\text{right}} = T_L$ ($T_H > T_L$). When applied to the heat-transfer unit, nonlinear perturbation represents the general heat-flow density, which can be introduced by nonlinear thermotics [13, 46] or be described as volumetric [42] convection or radiation, or heat exchange with the environment, which can be surface convection [43] or radiation thermal transmission [47,48]. Under the transformation $x' = L - x$, caused by the change of heat-flow direction, Eq. (1) can be expressed as

$$\frac{d}{dx'}\left(\kappa(L - x')\frac{dT}{dx'}\right) + \Phi\left(L - x', T, \frac{dT}{dx'}, \frac{d^2T}{dx'^2}, \cdots\right) = 0. \quad (2)$$

The boundary conditions are the same as those in Eq. (1). In one-dimensional and isotropic media, the solution of the two equations is symmetric about $T = (T_H + T_L)/2$ when $\Phi(x, T, dT/dx, d^2T/dx^2, \cdots) = 0$ in the one-dimensional case (see Supplemental Material [49] Note 1). When $\Phi(x, T, dT/dx, d^2T/dx^2, \cdots) \neq 0$, Eqs. (1) and (2) become nonlinear equations, so it is possible to produce unequal solutions under the transformation $x' = L - x$. Considering the nonlinear perturbation Φ as the general heat-flow density contributing to the heat-transfer element, there will be functional inequality when thermal rectification occurs:

$$\int_0^L \Phi\left(x, T, \frac{dT}{dx}, \frac{d^2T}{dx^2}, \cdots\right)dx \neq \int_0^L \Phi\left(L - x', T, \frac{dT}{dx'}, \frac{d^2T}{dx'^2}, \cdots\right)dx'. \quad (3)$$

As a sufficient necessary condition for the rectification phenomenon, the functional inequality indicates that asymmetric heat transfer is achieved when the nonlinear-perturbation term produces dissimilar feedback under the transformation $x' = L - x$. The presence of unequal solutions to Eqs. (1) and (2) may be inferred by comparing the forms of the two equations; this leads to the conclusion that $\kappa(L - x) \neq \kappa(x)$ [Fig. 1(c)] when the spatially dependent term of Φ is not congruent with the variation of κ. In Eqs. (1) and (2), considering isotropic media, analogous in format to $\nabla \cdot (\kappa_{\text{eff}}\nabla T) = 0$, the effective thermal conductivity

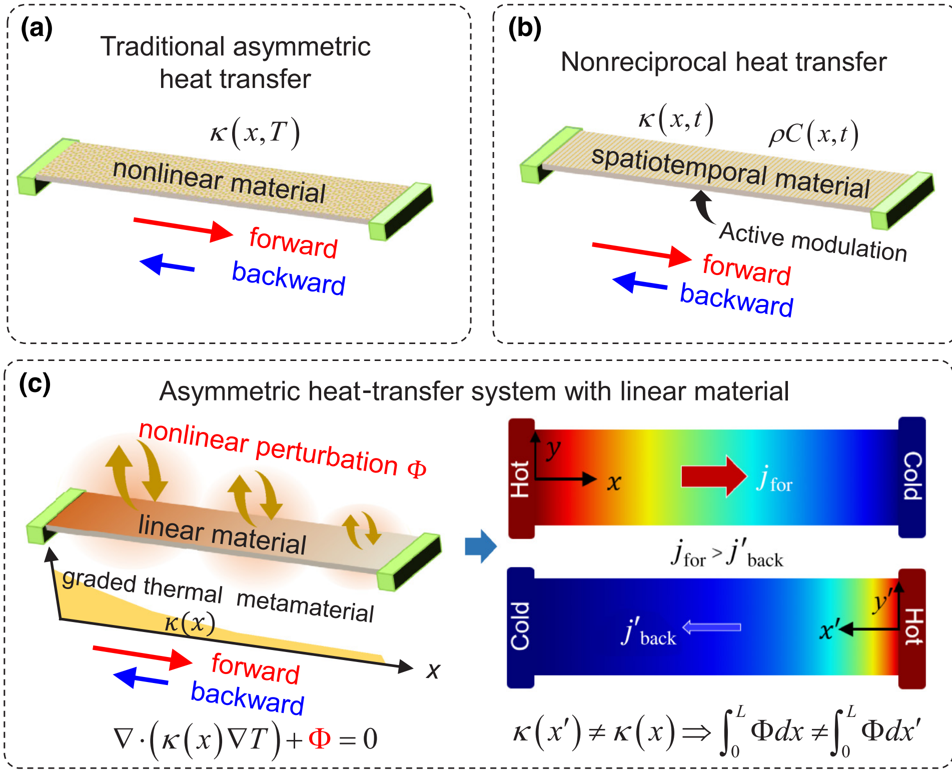

FIG. 1. Asymmetric heat-transfer system with linear conductive material. (a) Traditional asymmetric heat-transfer system with nonlinear conductive material. (b) Nonreciprocal heat-transfer system with spatiotemporal material. (c) Asymmetric heat-transfer system with graded linear conductive material tailors the nonlinear perturbation inserted into the heat-conduction equation and the asymmetric heat-transfer temperature profile with uneven transfer heat flow caused by asymmetric thermal conductivity.

of the system can be represented as

$$\kappa_{\text{eff}} = \kappa(x) + \psi\left(x, T, \frac{dT}{dx}, \frac{d^2T}{dx^2}, \ldots\right)\frac{dx}{dT}. \tag{4}$$

The divergence of the function $\Psi(x, T, dT/dx, d^2T/dx^2, \cdots)$ is $\Phi(x, T, dT/dx, d^2T/dx^2, \cdots)$,

$$\nabla\cdot\Psi\left(x, T, \frac{dT}{dx}, \frac{d^2T}{dx^2}, \ldots\right) = \Phi\left(x, T, \frac{dT}{dx}, \frac{d^2T}{dx^2}, \ldots\right). \tag{5}$$

The Gauss law can be applied to the left-hand side of Eq. (3) using Eq. (5), $\int \Phi dx = \Psi_{x=L} - \Psi_{x=0}$, which reflects the law of conservation of energy. It can be shown from Eqs. (4) and (5) that the nonlinear perturbation, Φ, will ultimately interact with the linear material parameters to produce a possible nonlinear effect and that nonlinear perturbation Φ is analogous to nonlinear thermal conductivity. For example, if nonlinear thermal conductivity [46] has the form $\kappa(x,T) = \kappa_X(x) + \kappa_T(T)$ or $\kappa(x,T) = \kappa_X(x)\kappa_T(T)$, the equivalent nonlinear-perturbation factors are $\Phi = \kappa_X(d^2T/dx^2) + (d\kappa_T/dT)(dT/dx)^2$ and $\Phi = (\kappa_X/\kappa_T)(d\kappa_T/dT)(dT/dx)^2$, respectively, and the heat-conduction equation transforms into

$$\frac{d}{dx}\left(\kappa_X(x)\frac{dT}{dx}\right) + \Phi = 0. \tag{6}$$

This equation demonstrates that the asymmetric response of the accompanying nonlinear perturbation on the heat-conduction equation is the essence of nonlinear thermal conductivity that could cause asymmetric heat transfer. The nonlinearization of thermal conductivity corresponds to the addition of an analogous heat source to traditional heat conduction, and the determination of the symmetry of the system still depends on the spatially dependent term $\kappa_X(x)$ of thermal conductivity. When $\kappa(L-x) \neq \kappa(x)$, which fulfills Eq. (3), asymmetric heat transfer with an uneven heat flux [Fig. 1(c)] can be achieved under the transformation $x' = L - x$. Naturally, it is also feasible to evaluate whether the system is asymmetric heat transfer by $\kappa_X(x)$ based on this conclusion when the thermal conductivity is nonlinear in the form of $\kappa(x,T) = \kappa_X(x) + \kappa_T(T)$ or $\kappa(x,T) = \kappa_X(x)\kappa_T(T)$. The system given by Eq. (6) displays the consequence of asymmetric heat transfer when $\kappa_X(L-x) \neq \kappa_X(x)$, which rectifies the misconception that

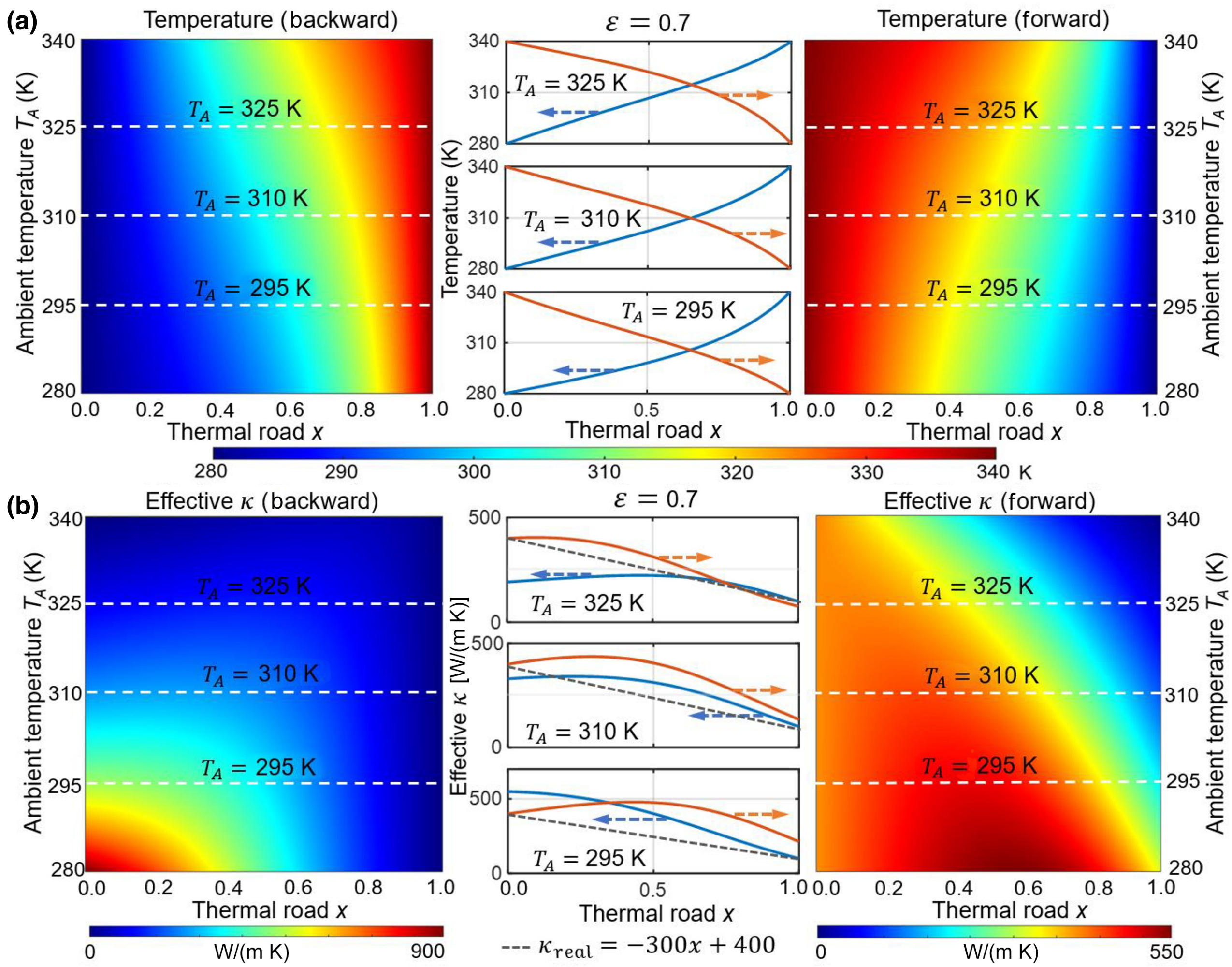

FIG. 2. Under transformation, $x' = L - x$, simulated asymmetric distribution of temperature (a) and effective thermal conductivity (b) at different ambient temperatures, T_A, while considering radiative heat transfer with an emissivity of $\varepsilon = 0.7$ and nonlinear perturbation Φ. Actual thermal-conductivity distribution with $\kappa_{\mathrm{real}} = -300x + 400$ [W/(m K), dark dashed line] when $\Phi = 0$.

results from disregarding the homogeneity of the functional space [15] (see Supplemental Material [49] Notes 2 and 3).

II. RESULTS AND DISCUSSION

To generate asymmetric heat transfer without employing nonlinear materials, the next stage is to assess the realizable nonlinear perturbation, Φ, and fulfill the sufficient necessary conditions for linear materials. We consider the surface-radiative heat-transfer and convective heat-transfer terms in a nonconservative heat-transfer system as a nonlinear-perturbation term. The independent effects of surface-radiation effects are first investigated. Under vacuum conditions, convective heat transfer is suppressed, and the surface-radiative heat of an inhomogeneous thermal-conductivity sheet of length L contributes solely to the nonlinear-perturbation term $\Phi = (2L/h)\varepsilon\sigma(T_A^4 - T^4)$, where $h \ll L$ is the thickness of the sheet, T_A is the ambient temperature, ε is the constant emissivity of the surface, and $\sigma = 5.67 \times 10^{-8}$ W/(m^{2}K^4) is the Stefan-Boltzmann constant. Equation (1) can be written as follows:

$$\frac{d}{dx}\left(\kappa(x)\frac{dT}{dx}\right) + \frac{2L}{h}\varepsilon\sigma(T_0^4 - T^4) = 0. \qquad (7)$$

In Eq. (7), it can be noted that the way the thermal conductivity is distributed determines whether or not asymmetric heat transfer is achievable. The solution of Eq. (7) is symmetric to $x = L/2$ with the same form of $T(x) = T'(L - x)$ when $\kappa(L - x) = \kappa(x)$, and this finding can also be exploited to construct the temperature-trapping device [21,50] (see Supplemental Material [49] Note 4). We investigate the dependence of asymmetry on how the thermal conductivity changes (see Supplemental Material [49] Note 5). The most obvious asymmetry occurs when thermal conductivity exists in a linear gradient manner. In the

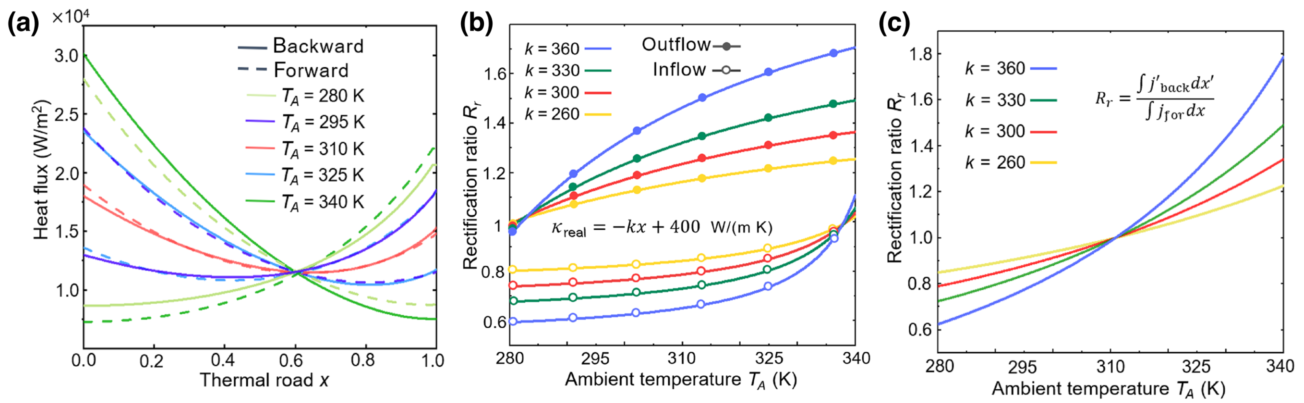

FIG. 3. (a) Radiative heat transfer with an emissivity of $\varepsilon = 0.7$ and nonlinear perturbation Φ, for heat flux distributions at different ambient temperatures under the forward and backward heat flows when the thermal conductivity is distributed with $\kappa_{\mathrm{real}} = -300x + 400$ W/(m K). (b) Rectification-ratio curves of heat inflow (solid dotted line) and outflow (hollow dotted line) under various linear parameters, k, of thermal conductivity, $\kappa_{\mathrm{real}} = -kx + 400$ W/(m K). (c) Rectification-ratio curves of average heat flow under various linear parameters, k, of thermal conductivity.

next analysis, the linear thermal-conductivity function is given the form $\kappa_{\mathrm{real}} = kx + b$, with $k = -300$ W/(m K) and $b = 400$ W/(m K).

Under various ambient temperatures, T_A, the simulated asymmetric distribution of temperature and effective nonlinear thermal conductivity produced by Eq. (5) is shown in Fig. 2. Under transformation $x' = L - x$, Eqs. (1) and (2) illustrate two distinct solutions, while their solutions are asymmetric about $T = (T_H + T_L)/2$ when $\Phi = 0$. For example, when $T_A = 295$, 310, or 325 K, the temperature distribution at all three temperatures is asymmetric at about $T = 310$ K. The effective nonlinear thermal conductivity, κ_{eff}, distribution does not overlap along the thermal road, which indicates that, with the inclusion of the nonlinear-perturbation factor, the equivalent thermal conductivity displays a temperature-interaction thermal conductivity comparable to that of the nonlinear thermal conductivity. Additionally, the temperature distribution is approximately symmetric due to the close value of the two effective thermal-conductivity curves at $T_A = 310$ K.

In Fig. 3, the mechanism of asymmetric heat transfer is explored, and the rectification efficiency of the structure under different ambient temperatures is investigated, by calculating the heat flux of forward and backward thermal transfer [Fig. 3(a)] and including the proportion of the inflow and outflow heat flows [Figs. 3(b) and 3(c)]. We calculate five distinct groups of heat fluxes in forward and backward directions at various ambient temperatures, T_A. As seen in Fig. 3(a), the heat-flow distribution is asymmetrical at the same ambient temperature, T_A. The heat inflow and outflow are not equal due to the out-of-plane heat exchange. Therefore, we individually compute the inflow and outflow rectification coefficients, $R_r = |j'_{\mathrm{back}}|/|j_{\mathrm{for}}|$, and display them in Fig. 3(c). It is observed that, at low ambient temperatures, inflow heat has the greatest rectification impact, whereas outflow heat flow has the greatest rectification impact at elevated temperatures. A larger thermal-conductivity slope value is beneficial when it comes to rectifying heat flow. In the present model with $k = 300$, it demonstrates that the rectification coefficient of outflow heat may surpass 1.37 when the ambient temperature is 340 K, and it can approach 0.73 when the ambient temperature is 280 K.

The experimental setup is schematically depicted in Fig. 4(a). Using the theory of neutral inclusions, the graded thermal metamaterial with a linear thermal conductivity, κ_{real}, that changes with slope k can be manufactured by filling the base-material plate with various materials following the rule $\kappa_{\mathrm{real}} = kx + b = \kappa_b + 3f(x)\kappa_b(\kappa_0 - \kappa_b)/(3\kappa_b + (1 - f(x))(\kappa_0 - \kappa_b))$, where κ_b and κ_0 are the thermal conductivity of the base material and the filling material, respectively, and f is the volume fraction of the filling material. The linear conductive metamaterials, as described in Fig. 4(a), are fabricated by mechanical punching and laser punching with 30×6 holes evenly punched in a 15×3 cm^2 area; each hole is located at the center of a 0.5×0.5 cm^2 area. A total of 15 groups of holes are used to obtain a linear thermal-conductivity function, $\kappa_{\mathrm{real}} = kx + \kappa_b$, by modulating the volume ratio, $f = \pi r^2/a^2$ ($r \in [0, 0.44]$ cm, $a = 0.5$ cm), occupied by each group of holes. To construct the equivalent thermal conductivity that is linearly changing, according to the value of $k = -300$ [i.e., $\kappa_{\mathrm{real}} \in [100, 400]$ W/(m K)], we use copper [$\kappa_b = 400$ W/(m K)] as the base material and cured epoxy resin [$\kappa_0 = 0.2$ W/(m K)] as the infill material. The graded thermal metamaterial, with a radiant heat-dissipation film with $\varepsilon = 0.7$, is placed in the vacuum chamber with an identical film attached to the inner walls to isolate the influence of thermal convection, leaving only the surface-radiative heat exchange between the sample and the surroundings. Under a temperature difference of 30–40 K, two heat-conduction conditions in the

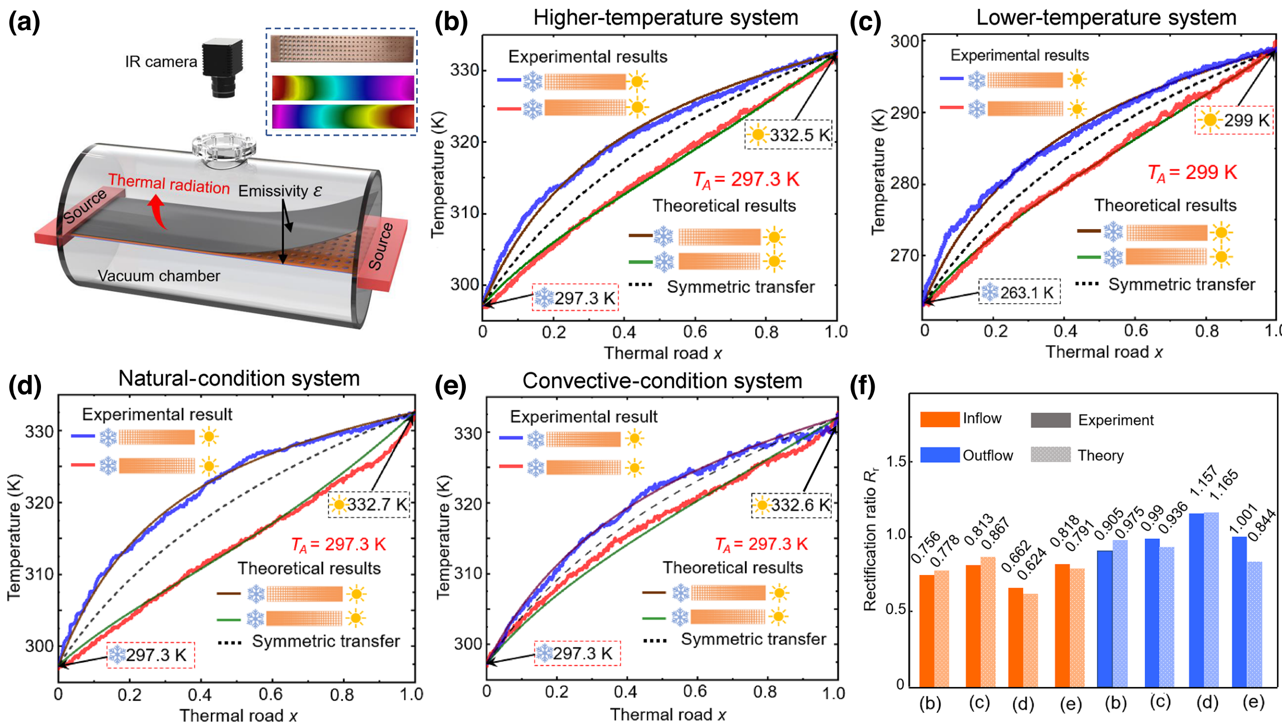

FIG. 4. Experimental verification of asymmetric heat-transfer system. (a) Radiant heat-dissipation film is applied to the front and back of the sample with a particular thermal-conductivity distribution and inserted in a vacuum chamber. Inset is a sample photograph and initial display of experimental results. Comparison between the results of experiment and theory under (b) $T_L = T_A = 297.3$ K, $T_H = 332.5$ K and (c) $T_H = T_A = 299$ K, $T_L = 263.1$ K, considering only the thermal-radiation condition ($\varepsilon_{\text{eff}} \approx 0.5$)and $k = 300$, $L = 0.15$ m, $h = 0.002$ m. Test component is seen in (b),(c) with holes of varying sizes in a sample. Heat conductivity decreases as the hole size increases. (d) Comparison between the results of experiment and theory under natural conditions, considering both thermal convection and radiation. (e) Calculated result considering only thermal convection. (f) Rectification coefficient derived from experimental and theoretical data.

forward and backward directions are examined for their temperature distributions, as shown in Figs. 4(b) and 4(c), by employing ambient temperature as the low-temperature end and the high-temperature end, respectively. The red experimental data adopt the original experimental values after transformation $x = 1 - x'$, whereas the blue data adopt the values after the $x = 1 - x'$ and $y = T_L + T_H - T_{\text{blue}}$ transformations to service the standard asymmetric heat-transfer effect. It indicates that, when $\Phi = 0$, the temperature-distribution curve after transformation is identical to the temperature-distribution curve without transformation (black dashed line), and when it is not equal to zero, there is a clear distinction. Both source-temperature systems are tested and compared under vacuum circumstances with theoretical values. The experimental results match well with theoretical values. In the higher-source-temperature system [Fig. 4(b)], the asymmetric impact is enhanced because the surface-radiation term takes the difference of the fourth-power form.

It is very difficult to determine the thermal-convection effect separately under the real challenge that the thermal-radiation impact is difficult to eliminate by experimental techniques. The approximate superposition property of thermal-radiation and thermal-convection effects followed in the heat-conduction equation is sufficient to characterize the result of asymmetric heat transfer only under convective conditions [Fig. 4(e)] by measuring the results of temperature profiles under natural conditions [Fig. 4(d)] at the same boundary conditions and eliminating the effect of thermal radiation. The superposition approximation can be represented as $T_c = T_s + (T_n - T_r)$, where T_c means the symmetric temperature (black dashed line); T_s and T_r represent the temperatures under convective [Fig. 4(e)] and radiative [Fig. 4(b)] conditions, respectively; and T_n represents the natural condition [Fig. 4(d)] considering both thermal convection and radiation. The calculated results for natural air convection under pure convection circumstances with a convective coefficient of 2 W/(m^2 K) correspond well with the theoretical outcomes.

The rectification coefficients of the heat inflow and outflow [Fig. 4(f)] are determined by fitting experimental data to the thermal conductivity at both ends. Even more convincing is that the experimental and theoretical rectification coefficients are in good agreement; this shows that the experiment is accurate from an even deeper perspective. When examining solely surface radiation, the high-temperature-system rectification impact is greater than that of the low-temperature system, which is consistent with the results in Figs. 4(b) and 4(c). Due to the weak thermal-convection coefficient under natural circumstances, the asymmetric heat-transfer impact considering just the thermal-convection effect is less than the asymmetric heat-transfer effect considering only the thermal-radiation effect. The nonlinear-perturbation excogitation theory provides a robust platform capable of exploiting the higher thermal-rectification coefficients sought by linear or nonlinear materials through bespoke nonlinear-perturbation terms, combined with corresponding graded thermal metamaterials with optimal gradients. In the context of this paper, it is feasible in further work to achieve optimal thermal rectification by the specific design of spatially dependent surface-radiation coefficients or thermal-convection coefficients that match the thermal conductivity of the linear-gradient distribution.

III. CONCLUSIONS

Incorporating nonlinear perturbations into the heat-conduction equation provides a straightforward perspective on the traditional passive asymmetric heat-transfer problem in the design of nonlinear materials. That is, the key to making asymmetric heat transfer with nonlinear thermal conductivity work is to make sure the asymmetry of their spatially independent parts is maintained. This theory offers a robust platform for the achievement of macroscopic asymmetries in heat transfer utilizing linear materials and employing graded thermal metamaterials. Proof-of-concept experiments considering surface radiation in a vacuum environment and considering both thermal radiation and convection, as well as the independent characterization of surface thermal convection using approximate superposition, proving the validity of the proposed asymmetric heat transfer. The nonlinear-perturbation model can add passive heat-related behavior to the heat-transfer equation. This means that asymmetric heat-transfer events can happen in volumetric radiation or convection transport systems that use graded thermal metamaterials. It is also possible to combine asymmetric heat-transfer events that involve, for example, thermoelectric effects. These discoveries provide a paradigm shift for asymmetric heat transfer, which could advance the developments of the thermal diode, the thermal rectifier, and other thermal metadevices.

ACKNOWLEDGMENTS

The present work was supported by the Fundamental Research Funds for the Central Universities (Grants No. HIT.OCEF.2021010 and No. 2021FZZX001-19) and the Young Scientist Workshop of Harbin Institute of Technology. Y.L. acknowledges support from the National Natural Science Foundation of China (Grants No. 92163123 and No. 52250191).

[1] B. Li, L. Wang, and G. Casati, Thermal Diode: Rectification of Heat Flux, Phys. Rev. Lett. **93**, 184301 (2004).

[2] C. W. Chang, D. Okawa, A. Majumdar, and A. Zettl, Solid-state thermal rectifier, Science **314**, 1121 (2006).

[3] L. Wang and B. Li, Thermal Logic Gates: Computation with Phonons, Phys. Rev. Lett. **99**, 177208 (2007).

[4] L. Wang and B. Li, Thermal Memory: A Storage of Phononic Information, Phys. Rev. Lett. **101**, 267203 (2008).

[5] M. Maldovan, Sound and heat revolutions in phononics, Nature **503**, 209 (2013).

[6] Xuan Chen, Min Li, Wenchao Chen, Haochen Yang, Zhicheng Pei, Er-Ping Li, Hongsheng Chen, Zuojia Wang, Broadband Janus scattering from tilted dipolar metagratings, Laser Photonics Rev. **16**, 2100369 (2022).

[7] F. Giazotto and M. J. Martínez-Pérez, The Josephson heat interferometer, Nature **492**, 401 (2012).

[8] M. J. Martínez-Pérez and F. Giazotto, A quantum diffractor for thermal flux, Nat. Commun. **5**, 3579 (2014).

[9] M. J. Martínez-Pérez, A. Fornieri, and F. Giazotto, Rectification of electronic heat current by a hybrid thermal diode, Nat. Nanotechnol. **10**, 303 (2015).

[10] S. Yuan, J. Yang, Y. Wang, Y. Chen, and X. Zhou, Highly sensitive temperature sensing via photonic spin Hall effect, Prog. Electromagn. Res. **177**, 21 (2023).

[11] N. A. Roberts and D. G. Walker, A review of thermal rectification observations and models in solid materials, Int. J. Therm. Sci. **50**, 648 (2011).

[12] M. Y. Wong, C. Y. Tso, T. C. Ho, and H. H. Lee, A review of state of the art thermal diodes and their potential applications, Int. J. Heat Mass Transfer **164**, 120607 (2021).

[13] G. Dai, J. Shang, R. Wang, and J. Huang, Nonlinear thermotics: Nonlinearity enhancement and harmonic generation in thermal metasurfaces, Eur. Phys. J. B **91**, 59 (2018).

[14] Y. Li, J. Li, M. Qi, C.-W. Qiu, and H. Chen, Diffusive nonreciprocity and thermal diode, Phys. Rev. B **103**, 014307 (2021).

[15] D. B. Go and M. Sen, On the condition for thermal rectification using bulk material, J. Heat Transfer **132**, 124502 (2010).

[16] G. Wehmeyer, T. Yabuki, C. Monachon, J. Wu, and C. Dames, Thermal diodes, regulators, and switches: Physical mechanisms and potential applications, Appl. Phys. Rev. **4**, 041304 (2017).

[17] M. Camacho, B. Edwards, and N. Engheta, Achieving asymmetry and trapping in diffusion with spatiotemporal metamaterials, Nat. Commun. **11**, 3733 (2020).

[18] J. Li, Y. Li, B. Li, P.-C. Cao, M. Qi, X. Zheng, Y.-G. Peng, X.-F. Zhu, A. Alù, H. Chen, and C.-W. Qiu, Reciprocity of thermal diffusion in time-modulated systems, Nat. Commun. **13**, 167 (2022).

[19] D. Torrent, O. Poncelet, and J.-C. Batsale, Nonreciprocal Thermal Material by Spatiotemporal Modulation, Phys. Rev. Lett. **120**, 12550 (2018).
[20] Y. Li, X. Shen, Z. Wu, J. Huang, Y. Chen, Y. Ni, and J. Huang, Temperature-Dependent Transformation Thermotics: From Switchable Thermal Cloaks to Macroscopic Thermal Diodes, Phys. Rev. Lett. **115**, 195503 (2015).
[21] X. Shen, Y. Li, C. Jiang, and J. Huang, Temperature Trapping: Energy-Free Maintenance of Constant Temperatures as Ambient Temperature Gradients Change, Phys. Rev. Lett. **117**, 055501 (2016).
[22] S. Kommandur, R. A. Kishore, C. Booten, S. Cui, L. M. Wheeler, and J. Vidal, Dual phase change thermal diodes with high rectification for thermal management near room temperature, Adv. Mater. Technol. **7**, 2101060 (2021).
[23] A. L. Cottrill, S. Wang, A. T. Liu, W.-J. Wang, and M. S. Strano, Dual phase change thermal diodes for enhanced rectification ratios: Theory and experiment, Adv. Energy Mater. **8**, 1702692 (2021).
[24] S. Narayana and Y. Sato, Heat Flux Manipulation with Engineered Thermal Materials, Phys. Rev. Lett. **108**, 214303 (2012).
[25] R. Schittny, M. Kadic, S. Guenneau, and M. Wegener, Experiments on Transformation Thermodynamics: Molding the Flow of Heat, Phys. Rev. Lett. **110**, 195901 (2013).
[26] C. Z. Fan, Y. Gao, and J. Huang, Shaped graded materials with an apparent negative thermal conductivity, Appl. Phys. Lett. **92**, 251907 (2008).
[27] S. Yang, J. Wang, G. Dai, F. Yang, and J. Huang, Controlling macroscopic heat transfer with thermal metamaterials: Theory, experiment and application, Phys. Rep. **908**, 1 (2021).
[28] Y. Li, W. Li, T. Han, X. Zheng, J. Li, B. Li, S. Fan, and C.-W. Qiu, Transforming heat transfer with thermal metamaterials and devices, Nat. Rev. Mater. **6**, 488 (2021).
[29] T. C. Han, X. Bai, D. Gao, J. T. L. Thong, B. Li, and C.-W. Qiu, Experimental Demonstration of a Bilayer Thermal Cloak, Phys. Rev. Lett. **112**, 054302 (2014).
[30] L. Wu, Cylindrical thermal cloak based on the path design of heat flux, J. Heat Transfer. **137**, 021301 (2015).
[31] H. Xu, X. Shi, F. Gao, H. Sun, and B. Zhang, Ultrathin Three-Dimensional Thermal Cloak, Phys. Rev. Lett. **112**, 054301 (2014).
[32] Y. Ma, Y. Liu, M. Raza, Y. Wang, and S. He, Experimental Demonstration of a Multiphysics Cloak: Manipulating Heat Flux and Electric Current Simultaneously, Phys. Rev. Lett. **113**, 205501 (2014).
[33] Y. Li, X. Bai, T. Yang, H. Luo, and C.-W. Qiu, Structured thermal surface for radiative camouflage, Nat. Commun. **9**, 273 (2018).
[34] T. Yang, Y. Su, W. Xu, and X. Yang, Transient thermal camouflage and heat signature control, Appl. Phys. Lett. **109**, 121905 (2016).
[35] Y.-G. Peng, Y. Li, P.-C. Cao, X.-F. Zhu, and C.-W. Qiu, 3D printed meta-helmet for wide-angle thermal camouflages, Adv. Funct. Mater. **30**, 2002061 (2020).
[36] X. He and L. Wu, Thermal transparency with the concept of neutral inclusion, Phys. Rev. E **88**, 033201 (2013).
[37] Y. Su, Y. Li, T. Yang, T. Han, Y. Sun, J. Xiong, L. Wu, and C.-W. Qiu, Path-dependent thermal metadevice beyond Janus functionalities, Adv. Mater. **33**, 2003084 (2021).
[38] T. Z. Yang, X. Bai, D. Gao, L. Wu, B. Li, J. T. L. Thong, and C.-W. Qiu, Invisible sensors: Simultaneous sensing and camouflaging in multiphysical fields, Adv. Mater. **27**, 7752 (2015).
[39] Y. Li, M. Qi, J. Li, P.-C. Cao, D. Wang, X.-F. Zhu, C.-W. Qiu, and H. Chen, Heat transfer control using a thermal analogue of coherent perfect absorption, Nat. Commun. **13**, 1 (2022).
[40] Y. Li, Y.-G. Peng, L. Han, M.-A. Miri, W. Li, M. Xiao, X.-F. Zhu, J. Zhao, A. Alù, S. Fan, and C.-W. Qiu, Anti-parity-time symmetry in diffusive systems, Science **364**, 170 (2019).
[41] Y. Li, K.-J. Zhu, Y.-G. Peng, W. Li, T. Yang, H.-X. Xu, H. Chen, X.-F. Zhu, S. Fan, and C.-W. Qiu, Thermal metadevice in analogue of zero-index photonics, Nat. Mater. **18**, 48 (2019).
[42] L. Xu, J. Wang, G. Dai, S. Yang, F. Yang, G. Wang, and J. Huang, Geometric phase, effective conductivity enhancement, and invisibility cloak in thermal convection-conduction, Int. J. Heat Mass Transfer **162**, 120659 (2021).
[43] R. Ju, G. Xu, L. Xu, M. Qi, D. Wang, P.-C. Cao, R. Xi, Y. Shou, H. Chen, C.-W. Qiu, and Y. Li, Convective thermal metamaterials: Exploring high-efficiency, directional, and wave-like heat transfer, Adv. Mater. **n/a**, 2209123 (2023).
[44] L. Xu, G. Dai, and J. Huang, Transformation Multithermotics: Controlling Radiation and Conduction Simultaneously, Phys. Rev. Appl. **13**, 024063 (2020).
[45] L. Xu, S. Yang, G. Dai, and J. Huang, Transformation omnithermotics: Simultaneous manipulation of three basic modes of heat transfer, ES Energy Environ. **7**, 65 (2020).
[46] S. R. Sklan and B. Li, A unified approach to nonlinear transformation materials, Sci. Rep. **8**, 4436 (2018).
[47] M. Peyrard, The design of a thermal rectifier, Europhys. Lett. **76**, 49 (2006).
[48] P.-C. Cao, Y. Li, Y.-G. Peng, M. Qi, W.-X. Huang, P.-Q. Li, and X.-F. Zhu, Diffusive skin effect and topological heat funneling, Commun. Phys. **4**, 230 (2021).
[49] See the Supplemental Material at http://link.aps.org/supplemental/10.1103/PhysRevApplied.20.034013 for more details about the relationship between the perturbation term and asymmetric heat transfer, as well as the discussion figures and experiment platform.
[50] L. Xu, J. Liu, P. Jin, G. Xu, J. Li, X. Ouyang, Y. Li, C.-W. Qiu, and J. Huang, Black-hole-inspired thermal trapping with graded heat-conduction metadevices, Natl. Sci. Rev. **10**, nwac159 (2023).